A SIMPLE DOA ESTIMATOR USING ADJACENT PATTERN POWER RATIO WITH SWITCHED BEAM ANTENNA

Y. Ozaki [1] **, J. Ozawa** [1] **, E. Taillefer** [2] **, J. Cheng** [1, *]**, and Y. Watanabe** [1]

[1]Department of Intelligent Information Engineering and Sciences, Doshisha University, Kyoto 610-0321, Japan

[2]Okinawa Institute of Science and Technology, Japan

Abstract—A simple DoA estimator is proposed with a switched beam antenna. The estimator is implemented with an adjacent pattern power ratio algorithm. For a single source signal, the received signal powers are measured while the antenna switches over a set of measured directive beam patterns. The pattern that exhibits the maximum received signal power is chosen. Then, the ratio between the pattern adjacent to the chosen pattern and the chosen pattern, is used to find the DoA by using a lookup table or by performing a linear regression approximation. Compared with conventional DoA estimators with switched beam antenna, the proposed algorithm allows DoA estimation with low computational cost, without sacrificing much the estimation precision. Computer simulations and experiments in an anechoic chamber are carried out to verify the proposed algorithm with a switched beam antenna: the electronically steerable parasitic array radiator (ESPAR) antenna.

1. INTRODUCTION

Direction of arrival (DoA) estimation which consists in estimating the bearing angle of an electromagnetic plane wave, is widely applied in wireless communication systems, environmental monitoring, channel sounding, radio astronomy, and so forth, and has received a significant amount of attention over the last several decades [1, 2].

An antenna array is commonly used for the DoA estimation of electromagnetic waves. It is well known that nearly all-existing antenna

arrays require one receiver chain per branch of antenna. Mobile user terminals have stringent limitations on hardware and algorithm complexity as well as power consumption. A single-port output array antenna, such as a switched beam antenna [3], is well suited for application to wireless communication systems, especially to mobile user terminals, since it requires little hardware.

Recently, conventional DoA estimation algorithms, such as MUSIC algorithm [4] and ESPRIT algorithm [5, 6], have been modified to be applied to switched beam antennas for DoA estimation [7–11]. Although these algorithms provide a high estimation precision, practical applications are difficult because of the high computational cost of eigen decomposition used in those algorithms.

For practical purposes, DoA estimation algorithms with low computational cost is desired for switched beam antennas. For a single source, several DoA estimation algorithms have be reported. An earlier direction-finding algorithm has been reported in [3, 12, 13]. The algorithm estimates the single DoA by switching multiple antenna beam patterns and by estimating the DoA as the direction corresponding to the maximum beam pattern. The resolution precision of the estimation depends on the number of beam patterns, and thus is coarse. A more accurate estimation has been also reported in [13] where the angle is determined by comparing the difference between the powers of received signals at each beam pattern with the pre-stored beam patterns correspond to these differences. However, DoA estimation based on the power difference could be influenced by the impinging signal strength.

On the other hand, a power pattern cross-correlation algorithm has been proposed, for a single source, to estimate DoA with a switched beam antenna [14]. The algorithm computes the cross-correlation coefficient between the measured antenna output power and stored beam patterns for several directions. Then, the direction giving the highest cross-correlation coefficient is taken as the estimated DoA. The algorithm give an accurate estimation. However, the cost of the cross-correlation coefficient computations increases with resolution of directions.

In this paper, we propose a simple DoA estimator with a switched beam antenna for a single signal. The estimator is implemented with an adjacent pattern power ratio (APPR) algorithm. In the algorithm, we measure the signal powers while the antenna switches over a set of directive beam patterns, and choose the pattern with the maximum signal power. Then, we calculate the adjacent pattern power ratio with respect to the maximum signal power pattern. We find the DoA by looking up a table (APPR-LT), in which the adjacent pattern

power ratios at the angle range near the maximum direction of the maximum signal power pattern are stored. Moreover, for further reduction of computational cost, instead of using a lookup table, we model a linear regression approximation (APPR-RA) to predict DoA. Computer simulations and experiments in an anechoic chamber are carried out to verify the proposed algorithm with a switched beam antenna: an electronically steerable parasitic array radiator (ESPAR) antenna.

The basic idea of the proposed APPR algorithm is similar to that in [13]. But we use adjacent pattern power ratio, rather than the power difference as in [13]. This avoids the influence of the strength of impinging signal on the estimation errors. Furthermore, compared with power pattern cross-correlation algorithm of [14], the proposed algorithm, especially APPR-RA, has low computational cost without much degradation on estimation precision.

This paper is organized as follows. Section 2 describes the adjacent pattern power ratio algorithm. Sections 3 and 4 give the simulation and experiment results with ESPAR antenna respectively. Finally in Section 5, the paper is summarized by conclusion remark.

2. ADJACENT PATTERN POWER RATIO ALGORITHM

In this section, we propose an adjacent pattern power ratio (APPR) algorithm for DoA estimation with a switched beam antenna. The algorithm is implemented by looking up a table (APPR-LT) in Section 2.1 or a regression approximation (APPR-RA) in Section 2.2.

2.1. APPR Algorithm with Lookup Table

For given N directive beam patterns $P_n(\psi)$, $(n = 1, 2, \ldots, N)$, we propose a simple DoA estimation algorithm. We call it adjacent pattern power ratio (APPR) algorithm. The N directive beam patterns can be obtained by a switched beam antenna [15], e.g., ESPAR antenna with reactance vectors $\mathbf{x}^{(n)}$, $(n = 1, 2, \ldots, N)$.

When considering a single signal impinging on the antenna at the unknown DoA θ, we estimate the DoA with the adjacent pattern power ratio algorithm as follows.

First, we measure the powers $\hat{P}_n(\theta)$, $n = 1, 2, \ldots, N$, of the received signal as the antenna switches the N directive beam patterns $P_n(\psi)$. The N measured powers $\hat{P}_n(\theta)$, $n = 1, 2, \ldots, N$, are used to estimate the DoA θ below.

Second, we choose the maximum power $P_{n^*}(\theta)$ among the N measured powers. Thus the DoA to be estimated is over about the

range $[\phi_{n^*} - \pi/N, \ \phi_{n^*} + \pi/N]$, where

$$n^* = \arg\max_n |\hat{P}_n(\theta)|.$$

Recall that in [12] the DoA θ was estimated to be ϕ_{n^*}. Although the complexity of the direction-finding algorithm of [12] is very low, obviously the DoA estimation is coarse. The estimation error depends on the number N of beam patterns.

Third, we introduce an *adjacent pattern power ratio* to improve the DoA estimation, compared with the directing-finding algorithm of [12]. For the maximum power $P_{n^*}(\theta)$, we define two adjacent pattern power ratios

$$\hat{\Gamma}_{n^*l}(\theta) = \frac{\hat{P}_{n^*}(\theta)}{\hat{P}_{n^*-1}(\theta)} \tag{1}$$

$$\hat{\Gamma}_{n^*r}(\theta) = \frac{\hat{P}_{n^*}(\theta)}{\hat{P}_{n^*+1}(\theta)}. \tag{2}$$

Notice that because of circular shift, $n^* + 1$ becomes 1 if $n^* = N$, and $n^* - 1$ becomes N if $n^* = 1$. Then, the estimation DoA $(\hat{\theta})$ is

$$\hat{\theta} \triangleq \psi^* = \begin{cases} \arg\min_{\psi} |\Gamma_{n^*l}(\psi) - \hat{\Gamma}_{n^*l}(\theta)| \\ \qquad \text{if } \hat{P}_{n^*+1}(\theta) < \hat{P}_{n^*-1}(\theta) \\ \arg\min_{\psi} |\Gamma_{n^*r}(\psi) - \hat{\Gamma}_{n^*r}(\theta)| \\ \qquad \text{if } \hat{P}_{n^*+1}(\theta) \geq \hat{P}_{n^*-1}(\theta) \end{cases} \tag{3}$$

where

$$\Gamma_{nl}(\psi) = \frac{P_n(\psi)}{P_{n-1}(\psi)} \tag{4}$$

$$\Gamma_{nr}(\psi) = \frac{P_n(\psi)}{P_{n+1}(\psi)}, \quad 0 \leq \psi < 2\pi \tag{5}$$

are the ratio of the two adjacent pattern powers, which are prepared prior to a practical DoA estimation. The upper part of (3) means that when the DoA falls into the left side of the n^*-th pattern (i.e., $\hat{P}_{n^*+1}(\theta) < \hat{P}_{n^*-1}(\theta)$), for a given $\hat{\Gamma}_{n^*l}(\theta)$ we estimate the DoA ψ^* such that the values of $\Gamma_{n^*l}(\psi)$ and $\hat{\Gamma}_{n^*l}(\theta)$ is the nearest.

In practice, we implement (3) by using a lookup table to reduce run-time computations. The values of $\Gamma_{nl}(\psi)$ $(\phi_n - \pi/N \leq \psi < \phi_n)$ and $\Gamma_{nr}(\psi)$ $(\phi_n \leq \psi < \phi_n + \pi/N)$ are prepared and stored as a table. We look up into the table $\Gamma_{nl}(\psi)$ or $\Gamma_{nr}(\psi)$, depending on if the comparison is with $\hat{P}_{n^*-1}(\theta)$ or $\hat{P}_{n^*+1}(\theta)$.

2.2. APPR Algorithm with Regression Approximation

Although the complexity of the APPR-LT algorithm is low, the computational complexity and the amount of memory required for storing the table of adjacent pattern power ratio, in the third step of the algorithm, can be further reduced. For this purpose, we propose an estimation algorithm based on the adjacent pattern power ratio with regression approximation.

Instead of the lookup table in the adjacent pattern power ratio algorithm stated in Section 2.1, here we propose a linear regression equation to estimate the DoA.

For the ratio $\Gamma_{nl}(\psi)$ of the two adjacent pattern powers, we give a linear regression equation

$$\hat{\psi} = a_{nl} \cdot \Gamma_{nl}(\psi) + b_{nl} + \phi_n \qquad (6)$$

to predict the DoA for a given power ratio Γ_{nl}. The regression coefficients a_{nl} and b_{nl} are modeled, by the least square function, from the sample values at different directions $\phi_n - \pi/N \leq \psi < \phi_n$. Similarly, a linear regression equation

$$\hat{\psi} = a_{nr} \cdot \Gamma_{nr}(\psi) + b_{nr} + \phi_n \qquad (7)$$

is used to predict the DoA for a given power ratio Γ_{nr}. In the simulation we assume that $a_{nl} = a_l$, $b_{nl} = b_l$, $a_{nr} = a_r$, $b_{nr} = b_r$ because of the symmetry of the antenna.

We are now ready to describe the adjacent pattern power ratio algorithm with a regression approximation (APPR-RA). The approximate estimation is obtained from the linear regression equations. After measuring the N powers and choosing the maximum power $P_{n^*}(\theta)$, as we stated in Section 2.1, we estimate the DoA by using the following linear regression equations

$$\hat{\theta}\ [^\circ] = \begin{cases} a_l \cdot \hat{\Gamma}_{n^*l}(\theta) + b_l + \phi_{n^*} \\ \qquad \text{if } \hat{P}_{n^*+1}(\theta) < \hat{P}_{n^*-1}(\theta) \\ a_r \cdot \hat{\Gamma}_{n^*r}(\theta) + b_r + \phi_{n^*} \\ \qquad \text{if } \hat{P}_{n^*+1}(\theta) \geq \hat{P}_{n^*-1}(\theta). \end{cases}$$

The adjacent pattern power ratio algorithm with regression approximation (APPR-RA) estimate the DoA by calculating its linear regression equation, and thus, compared with the PPCC algorithm in [14], APPR-RA has a low computational complexity. Because PPCC requires to calculate the correlation coefficient between the measured powers and the power patterns at all the direction from $0°$ to $360°$, therefore, the computational complexity increases with the increase of the resolution.
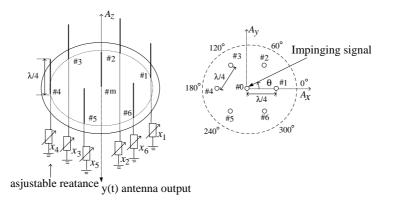
3. SIMULATIONS

This section describes some simulations of the APPR algorithms with a switched beam antenna, the ESPAR antenna.

3.1. A Switched-beam Antenna: ESPAR Antenna

The ESPAR antenna, as an example of switched beam antenna, features a simple hardware structure, which enables the use of switched beam antenna techniques to user terminals in wireless applications [16, 18]. An $(M+1)$-element ESPAR antenna with $M = 6$ is depicted in Fig. 1. The 0-th element is an active radiator located at the center of a circular ground plane. It is a 0.25λ-monopole (where λ is the wavelength) and is excited from the bottom in a coaxial fashion. The remaining M elements of 0.25λ-monopoles are passive radiators surrounding the active radiator symmetrically with the radius 0.25λ of the circle. Each of these elements is terminated by a variable reactance $\mathbf{x}_m$, $(m = 1, 2, \ldots, M)$. In practical applications, the value of reactance may be constrained in certain ranges, e.g., from $-300\ \Omega$ to $300\ \Omega$. The vector denoted by

$$\mathbf{x} = [x_1, x_2, \ldots, x_M]^{\mathrm{T}}$$

is called the reactance vector, which is variable, and thus is used to form an antenna pattern. Here the superscript $^{\mathrm{T}}$ is the transpose of the vector or matrix. We will see in Section 3.3 that a directive pattern can be formed by a given reactance vector. Note that in a fabricated ESPAR antenna, the value of reactance x_i is adjusted by a bias voltage on the reactance. Variable antenna pattern occurs by controlling the bias voltages, and thus the values of reactances.

Figure 1. (a) Diagram of ESPAR antenna, (b) 7-element ESPAR antenna.

3.2. Signal model of ESPAR antenna

Consider the case of a single signal $s(t)$. When $s(t)$ is from the DoA θ, the output of ESPAR antenna can be expressed [14]

$$y(t) = \boldsymbol{w}^{\mathrm{T}}\boldsymbol{a}(\theta)s(t) + n(t) \tag{8}$$

where $n(t)$ is an additive white Gaussian noise, and $\mathbf{a}$ is a steering vector

$$\boldsymbol{a}(\theta) = \left[1, e^{j\frac{\pi}{2}\cos(\theta-\Psi_1)}, ..., e^{j\frac{\pi}{2}\cos(\theta-\Psi_M)} \right]^{\mathrm{T}} \tag{9}$$

with $\Psi_m = \frac{2\pi}{M}(m-1)$, $(m = 1, ..., M)$. Here $\mathbf{w}$ is the RF current vector

$$\mathbf{w} = 2V_s(\mathbf{Z} + \mathbf{X})^{-1}\mathbf{u}_0 \tag{10}$$

where the diagonal matrix $\mathbf{X} = \mathrm{diag}\{z_0, jx_1, ..., jx_M\}$ is the reactance matrix, $\boldsymbol{u_0} = [1, 0, 0, 0, 0, 0, 0]^{\mathrm{T}}$ is an $(M + 1)$ components vector and V_s is a constant. The $(M + 1) \times (M + 1)$ constant matrix $\mathbf{Z}$ is the mutual impedance matrix. The values of the components in $\mathbf{Z}$ depend on the physical structure of the antenna, e.g., the radius, the element spacing and the lengths of the elements, and therefore are constant for a given fabricated antenna [9]. Note that during the simulations the power $\hat{P}_n(\theta)$ is estimated from the output $y(t)$ of the antenna as

$$\hat{P}_n(\theta) = \frac{1}{L}\sum_{\ell=1}^{L}|y(\ell)|^2. \tag{11}$$

3.3. Six Directive Beam Patterns

According to the structure of ESPAR antenna (see Fig. 1), the reactance loaded in each of the parasitic elements electronically adjusts its element length and makes the monopole element appear as a director or a reflector, similarly to a Yagi-Uda array antenna [3], depending on the negative or positive value of the reactance. The element appears as an effectively 'shorter' monopole (director) if a negative reactance is loaded, while a positive reactance provides an effectively 'longer' element (reflector). This action of the loaded reactance causes a change in the radiation pattern.

Following the basic principle of Yagi-Uda array antenna above, to from a directive beam pattern to a given direction, it is obvious that the elements toward to the direction should be loaded with negative reactances, and act as director, while the elements at the opposite direction should be loaded with positive reactances, and act as reflector. For example, to form a beam to direction $0°$, the elements

1, 2 and 6 (see $\phi_1 = 0°$ in Fig. 1) should be loaded with the minimum reactance, i.e., $-300\,\Omega$, while the remaining elements should be loaded with the maximum reactance $300\,\Omega$. Thus we obtain a directive beam pattern toward to direction $0°$ (see Fig. 2) from the calculation of (8).

Due to the symmetry of the ESPAR antenna, the directive beam pattern obtained by rotating the pattern by $60°$ ($2\pi/M$ in radian) is the same as that obtained by rotating the reactance values. The six directive beam patterns are shown in Fig. 2, and their corresponding reactances are given in Table 1.

For convenience, we denote as $P_n(\psi)$, ($0 \leq \psi < 2\pi$) the n-th directive beam pattern having a corresponding reactance vector $\mathbf{x}^{(n)}$, $n = 1, 2, \ldots, N$. The maximum gain of the pattern is toward the direction angle $\phi_n = 2\pi(n-1)/N$. Here N is the number of directive beam patterns. In this paper, as an example, we take $N = M = 6$. But, the proposed DoA estimation algorithm is not limited to $N = M$.
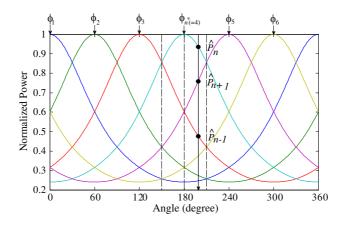

Figure 2. Six directive beam patterns.

Table 1. Reactance values for beam patterns of Fig. 2.

directions	x_1	x_2	x_3	x_4	x_5	x_6
0°	−300	−300	300	300	300	−300
60°	−300	−300	−300	300	300	300
120°	300	−300	−300	−300	300	300
180°	300	300	−300	−300	-300	300
240°	300	300	300	−300	−300	−300
300°	−300	300	300	300	−300	−300

For the APPR-RA algorithm, the regression coefficients in (6) and (7) in our simulations are $a_l = 45.45$, $a_r = -45.45$, $b_l = -75.45$, and $b_r = 75.22$, which are modeled from the samples of $\Gamma_{nl}(\psi)$ in (5) and $\Gamma_{nr}(\psi)$ in (4) with an angle increment of $1°$. The regression lines with the samples of $\Gamma_{nl}(\psi)$ and $\Gamma_{nr}(\psi)$ are shown in Fig. 3 with $n = 2$.

3.4. Simulation Results

During the simulations, a 7-element ($M = 6$) ESPAR antenna is employed as a switched beam antenna with $N = 6$ directive beam patterns. The modulation scheme for the signal $s(t)$ in (8) is binary phase shift keying (BPSK). The binary symbols are uniformly distributed. The signal-to-noise power is 20 dB. Without a specific declaration, the data block size for each calculation of the power defined in (11) is taken to be $L = 100$. The simulation parameters are given in Table 2.
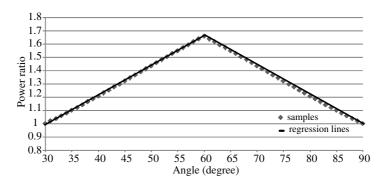

Figure 3. Regression lines and samples of $\Gamma_{nl}(\psi)$ ($30° \leq \psi < 60°$) and $\Gamma_{nr}(\psi)$ ($60° \leq \psi < 90°$) with an angle increment of $1°$ ($n = 2$) (Simulation).

Table 2. Simulation parameter.

Number of patterns	$N = 6$
Data modulation	BPSK
Signal samples	$N \times L$
DoA range	$[0,\ 60]°$
Signal to noise power	20 dB
Increment of DoA	$1°$

When the signal impinges on the antenna at the unknown DoA θ, we estimate the DoA and calculate the estimation error. Due to the symmetry of ESPAR antenna, we only consider the DoA from the range over $[0, 60]°$. DoA estimations are carried out when DoA is with an angle increment of $1°$. The estimation error for the by APPR-LT method are shown in Fig. 4. The average estimation error for APPR-LT is $1.5°$. Fig. 5 shows the estimation error for the APPR-RA method, where the average estimation error is $1.7°$. For comparison, we also give the estimation error for the PPCC method (see Fig. 6), where the average estimation error is $1.1°$.

The statistic performance, i.e., the mean and standard deviation (std), of the estimation error is summarized in Table 3. APPR-RA with $L = 100$ has almost the same error mean as APPR-LT. And, compared with PPCC, APPR-RA does not bring significant estimation precision
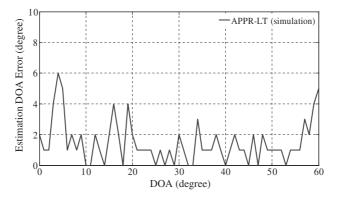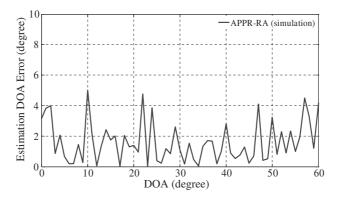

Figure 4. Estimation errors by APPR-LT (simulation).

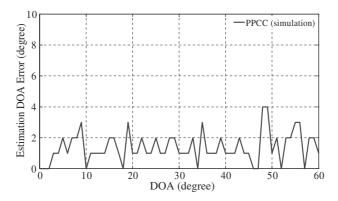**Figure 5.** Estimation errors by APPR-RA (simulation).

Figure 6. Estimation errors by PPCC (simulation).

Table 3. Compare to simulation of DoA estimation error between APPR-LT, -RA, and PPCC (SIMULATION).

		$L = 20$	$L = 50$	$L = 100$
APPR-LT	mean	3.6°	2.1°	1.5°
	std	3.4°	2.6°	2.4°
APPR-RA	mean	3.4°	2.3°	1.7°
	std	3.4°	2.6°	2.4°
PPCC	mean	2.4°	1.5°	1.1°
	std	2.5°	2.5°	1.4°

degradation. Notice that, as we stated in Section 2.2, compared with PPCC, APPR-RA has a low computational cost.

4. EXPERIMENTS

This section reports DoA estimation experiments using the proposed APPR algorithms with the ESPAR antenna.

4.1. A Prototype of ESPAR Antenna and Its Directive Beam Patterns

Figure 7 shows a prototype of the 2.484 GHz ESPAR antenna used for the experiments. Each parasitic element is loaded with a variable reactance x. A digital voltage ranging between -2048 and 2047 is converted into an analog bias voltage, which adjusts the value of each reactance. When the bias voltage varies from 20 to -0.5 V, according

to the 1SV287 diode specifications, the reactive loading provides a reactance varying over -45.8 to $-3.6\,\Omega$. The reactance loaded in the parasitic element electronically adjusts the element's length and makes the monopole appear as a director or a reflector, depending on the value of the reactance. Thus, this action of the loaded reactances causes a change in the radiation pattern. The six beam patterns, used in these experiments, are shown in Fig. 8. These pattern was formed by a single-source power maximum algorithm proposed in [17].

Table 4 gives six sets of the regression coefficients. The n-th set is modeled from the samples of $\Gamma_{nl}(\psi)$ in (4) and $\Gamma_{nr}(\psi)$ in (5) with an angle increment of $1°$ for the given antenna patterns shown in Fig. 8. The regression lines with the samples of $\Gamma_{nl}(\psi)$ and $\Gamma_{nr}(\psi)$ are shown in Fig. 9 with $n = 2$.
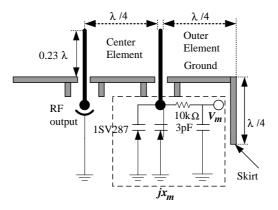

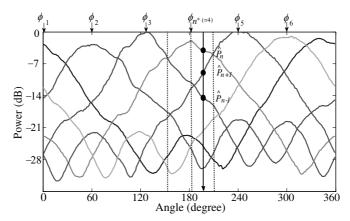**Figure 7.** Cross-section of ESPAR antenna circuit.
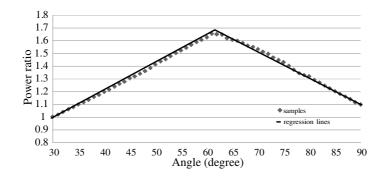

Figure 8. Measured directive beam pattern.

Figure 9. Regression lines and samples of $\Gamma_{nl}(\psi)$ $(30° \leq \psi < 60°)$ and $\Gamma_{nr}(\psi)$ $(60° \leq \psi < 90°)$ with an angle increment of $1°$ $(n = 2)$ (Experiment).

Table 4. The regression coefficients in experiments.

	a_l	b_l	a_r	b_r
$n = 1$	90.90	−89.36	−45.45	73.59
$n = 2$	47.61	−46.23	−50.00	85.25
$n = 3$	47.61	−45.61	−66.66	102.13
$n = 4$	83.33	−83.58	−58.82	82.64
$n = 5$	66.66	−65.60	−66.66	99.46
$n = 6$	90.90	−89.90	−100.00	128.70

4.2. Experiment Results

The experiment took place in an anechoic chamber using the setup shown in Fig. 10. The transmitter is a Horn antenna, and the transmitting signal data are modulated and generated from a signal generator (SG) fed by an M-sequencer. The RF receiver gets a signal from the ESPAR antenna output and provides demodulated quadratic and in-phase signals to a digital signal processor (DSP)-based controller. This DSP is used to convert the analog signals (with 12-bit resolution) to digital signals and also provides the observed data.

The experiment parameters are given in Table 5. We consider the DoA from the range over $[0, 350]°$. DoA estimations are carried out when DoA is with an angle increment of $10°$ against signals in 36 directions of total.

The estimation errors by APPR-LT, -RA and PPCC are shown in Fig. 11. The average estimation error is $2.1°$. Fig. 11 shows the
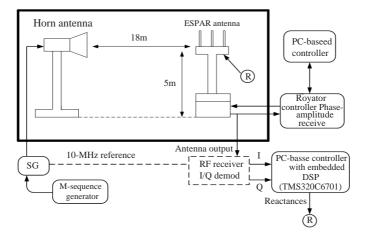
Figure 10. Experimental environment and measurement system setup.

Table 5. Experimental parameters.

RF frequency of impinging signal	2.484 GHz
Number of patterns	$N = 6$
Data modulation	BPSK
Number of received signal samples	$N \times L$
DoA range	$[0, \ 350]°$
Estimated noise level	20 dB
Power of impinging signal	10 dBm
Increment of DoA	$10°$

Table 6. Compare of DoA estimation error between APPR-LT, -RA, and PPCC (Experiment).

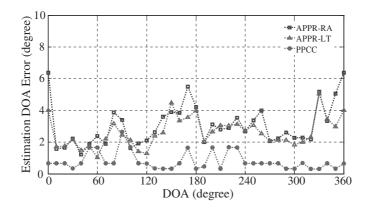|		$L = 20$	$L = 50$	$L = 100$
APPR-LT	mean	2.6°	2.1°	2.1°
	std	2.6°	2.4°	2.4°
APPR-RA	mean	2.9°	2.8°	2.8°
	std	2.6°	2.4°	2.4°
PPCC	mean	1.4°	1.3°	1.3°
	std	1.2°	1.2°	1.2°

Figure 11. Estimation errors by APPR-LT, -RA and PPCC (experiment).

estimation error by APPR-RA, where the average estimation error is 2.8°. For comparison, we also give the estimation error when employing the PPCC algorithm (see Fig. 11), where the average estimation error is 1.3°.

5. CONCLUSION

We proposed an adjacent pattern power ratio (APPR) algorithm to estimate DoA with switched beam antenna. For a single source, the signal powers are measured as the antenna switches over a set of directive beam patterns. The pattern with the maximum signal power is chosen. Then the adjacent pattern power ratio with respect to the maximum signal power pattern is used to find the DoA by looking up into a table or a linear regression approximation. The proposed algorithm provides a simple DoA estimator with low computational cost. Simulations and experiments show that compared to the conventional DoA estimation for switched beam antenna, the proposed algorithm can provide accurate DoA estimation without significantly degrading the estimation precision.

REFERENCES

1. Johnson, D. H. and D. E. Dudgeon, *Array Signal Processing, Concepts and Techniques*, Signal Processing Series, PTR Prentice-Hall, 1993.

2. Chandran, S., *Advances in Direction-of-Arrival Estimation*, Artech House, Inc., Boston, 2005.

3. Thiel, D. V. and S. Smith, *Switched Parasitic Antennas for Cellular Communications*, Artech House, Inc., Boston, 2001.

4. Schmidt, R. O., "Multiple emitter location and signal parameter estimation," *IEEE Trans. on Antennas and Propagation*, Vol. 34, 276–280, Mar. 1986.

5. Roy, R. and T. Kailath, "ESPRIT- estimation of signal parameters via rotational invariance techniques," *IEEE Trans. on Acoustics, Speech, and Signal Processing*, Vol. 37, No. 7, 984–995, Jul. 1989.

6. Taillefer, E., J. Cheng, and Y. Watanabe, "Full azimuth direction-of-arrival estimation with successive-selection technique," *IEEE Trans. on Signal Processing*, Vol. 56, No. 12, 5903–5915, Dec. 2008.

7. Svantesson, T. and M. Wennstrom, "High-resolution direction finding using a switched parasitic antenna," *11th IEEE Signal Processing Workshop on Statistical Signal Processing*, 508–511, Singapore, Aug. 2001.

8. Plapous, C., J. Cheng, E. Taillefer, A. Hirata, and T. Ohira, "Reactance domain MUSIC algorithm for electronically steerable parasitic array radiator," *IEEE Trans. on Antennas and Propagation*, Vol. 52, No. 12, 3257–3264, Dec. 2004.

9. Cheng, J. and T. Ohira, "ESPAR antenna signal processing for DoA estimation," *Advances in Direction-of-Arrival Estimation*, 395–417, Ed. by Sathich Chandran, Artech House, Inc., Boston, Dec. 2005.

10. Varlamos, P. K., S. A. Mitilineos, S. C. Panagiotou, A. I. Sotiriou, and C. N. Capsalis, "Direction-of-Arrival estimation approach using switched parasitic arrays," *Advances in Direction-of-Arrival Estimation*, 145–160, Ed. By Sathich Chandran, Artech House, Inc., Boston, Dec. 2005.

11. Taillefer, E., W. Nomura, J. Cheng, M. Taromaru, Y. Watanabe, and T. Ohira, "Enhanced reactance-domain ESPRIT algorithm employing multiple beams and translational-invariance soft selection for direction-of-arrival estimation in the full azimuth," *IEEE Trans. on Antennas and Propagation*, Vol. 56, No. 8, 2514–2526, Aug. 2008.

12. Ohira, T. and K. Gyoda, "Hand-held microwave direction-of-arrival finder based on varactor-tuned analog aerial beam-forming," *Proc. Asia-Pacific Microwave Conf.*, 585–588, Taipei, Dec. 2001.

13. Preston, S. T., D. V. Thiel, T. A. Smith, S. G. O'Keefe, and J. Lu, "Base-station tracking in mobile communications using a switched parasitic antenna array," *IEEE Trans. on Antennas and Propagation*, Vol. 46, No. 6, 841–844, Jun. 1998.

14. Taillefer, E., A. Hirata, and T. Ohira, "Direction-of arrival estimation using radiation power pattern with an ESPAR antenna," *IEEE Trans. on Antennas and Propagation*, Vol. 53, No. 2, 678–684, Feb. 2005.

15. Ozaki, Y., J. Ozawa, E. Taillefer, J. Cheng, and Y. Watanabe, "Direction-of-arrival estimation using adjacent pattern power ratio with switched beam antenna," *IEEE Pacific Rim Conference on Communications, Computer and Signal Processing (PacRim)*, 453–458, Aug. 2009.

16. Cheng, J., M. Hashiguchi, K. Iigusa, and T. Ohira "Electronically steerable parasitic array radiator antenna for omni- and sector pattern forming applications to wireless ad hoc networks," *IEE Proc. - Microw. Antennas and Propag.*, Vol. 150, No. 4, 203–208, Aug. 2003.

17. Cheng, J., E. Taillefer, and T. Ohira, "Omni-, sector and adaptive modes of compact array antenna," *Handbook on Advancements in Smart Antenna Technologies for Wireless Networks*, C. Sun, J. Cheng, and T. Ohira (eds.), 532–544, IGI Global, Hershey, USA, 2008.

18. Ohira, T. and K. Iigusa, "Electronically steerable parasitic array radiator antenna," *The Transactions of the Institute of Electronics, Information and Communication Engineers, C*, Vol. J87-C, No. 1, 12–31, Jan. 2004 (in Japanese).